

GEOCHEMICAL CHARACTERIZATION OF HEAVY METALS AND ENVIRONMENTAL RISK ASSESSMENT OF ROAD DUST IN CAIRO, EGYPT

Hanan H. Ghareeb^{(1)*}; Fayza S. Hashem⁽²⁾; Ragab M. Maree⁽³⁾;
Mahmoud A. I. Hewehy⁽¹⁾

1) Environmental Basic Sciences Department, Faculty of Environmental Studies and Research, Ain Shams University 2) Chemistry Department, Faculty of Science, Ain Shams University, Cairo, Egypt 3) Radiation Protection Department, Atomic Energy Authority, Egypt

*Corresponding author: Hanan Hegazy G. Email: Geohanan1@gmail.com

ABSTRACT

Urban road dust pollution is a significant issue contributing to atmospheric pollution and storing contaminants such as heavy metals. This study aims to determine the heavy metal content and spatial distribution of road dust in Cairo, a city with increased anthropogenic activity, and to identify the possible main sources of individual metals using multivariate statistical analysis. Our study utilized inductively coupled plasma-mass spectroscopy (ICP-MS) to assess samples containing 15 heavy metal forms, including Chromium (Cr), Zinc (Zn), Arsenic (As), Cadmium (Cd), Mercury (Hg), Lead (Pb), Cobalt (Co), Bismuth (Bi), Nickel (Ni), Copper (Cu), Gallium (Ga), Strontium (Sr), Silver (Ag), Indium (In), Barium (Ba), and Iron (Fe). Various geo-accumulation indices, contamination factors, degree of contamination, pollution load index, enrichment factor, and pollution ecological risk index were used to evaluate the pollution degree. Results showed that the mean concentrations of the major heavy metals were 1798.55, 396.3, 410.22, 466.39, and 472.81 ppm for Pb, Bi, Ni, Cu, and Zn, respectively. The heavy metal spatial distribution was site-specific, with high Bi levels due to extensive industrial activities. The pollution degree decreased in the order of Bi > Hg > Cd > Zn > In > As > Cu. The heavy metals ranged from non-polluting to highly polluting. The study suggested that Bi substitutes Pb in the manufacturing industry as it poses lower risks. The toxic response (Tr) should be figured out regarding its significant enrichment.

Keywords: Road dust; Pollution Indices; Heavy metals; Environmental assesemnt; Bismuth (Bi)

INTRODUCTION

Urban regions globally are undergoing swift transformation due to rampant urbanization, vigorous human activities, industrialization, persistent need for land for infrastructure expansion, and rapid growth of the social economy. As a result, the urban

environment experiences a decrease in quality (Abbasi *et al.*, 2017). A prevalent type of air pollution that has become widespread globally is road dust contamination. Urban regions have been experiencing a recent rise in road dust contamination due to industrial and road traffic activity (Ferreira-Baptista and De Miguel, 2005; Abdellatif and Saleh, 2012). The problem of urban road dust pollution has become a significant worry in recent years. This is mainly because urban road dust can serve as a source of materials contributing to air pollution through resuspension. Additionally, they can also temporarily accumulate contaminants such as heavy metals and polycyclic aromatic hydrocarbons. Dust particles typically have diameters ranging from around 1 to 100 μm and descend gradually due to the force of gravity (Calvert, 1990). The accumulation of dust on surfaces, particularly along roadsides, is referred to as road dust. This dust is contaminated with various heavy metals, including Arsenic (As), Cadmium (Cd), Cobalt (Co), Chromium (Cr), Copper (Cu), Mercury (Hg), Manganese (Mn), Nickel (Ni), Lead (Pb), Antimony (Sb), Strontium (Sr), and Zinc (Zn), as well as certain organic substances (Han *et al.*, 2017). Traffic emissions arise from releasing exhaust particles from vehicles and particles generated by tire wear, weathered street surfaces, and brake lining wear. Industrial emissions, on the other hand, are emitted by industrial power plants, coal combustion, metallurgical industry, auto repair shops, chemical plants, and similar sources. A profound correlation exists between environmental contamination of trace elements (TE) and human exposure (Meza-Figueroa *et al.*, 2007). Moreover, Alzheimer's, diabetes, and atherosclerosis are human diseases associated with the presence of heavy metal pollution (Yang *et al.*, 2018; Mitra *et al.*, 2022).

The swift process of urbanization, along with the advancement of the social economy, results in the expansion of transportation networks both within and beyond major urban areas. The presence of heavy metals in road dust near urban roadways is influenced by various factors, including (i) the density of road traffic and the distance from the road; (ii) the proximity of industrial establishments to the road (Trujillo-González *et al.*, 2016; Gabarrón *et al.*, 2017; Wang *et al.*, 2020). In addition, several factors, such as topography, construction projects, and proximity to rivers, influence the concentration of heavy metals in road dust (Duong and Lee, 2011). Industrial areas exhibit higher levels of TE in road dust

compared to residential and commercial districts (El-Anwar *et al.*, 2018; Olmedo *et al.*, 2018; Ramírez *et al.*, 2019). Cairo is an expanding metropolis experiencing tremendous growth in all directions. It is surrounded by numerous industrial zones, resulting in various environmental challenges for the city. Cairo has an area of approximately 214.2 km², extending along the shores of the River Nile. The roadway dust in Cairo is exposed to different amounts of human-made metals from different sources that can be either mobile or stationary. These sources include vehicular traffic, industrial plants, power generation facilities, residential oil burning, waste incineration, construction and demolition activities, and the resuspension of contaminated soils in the surrounding areas. Pollution ecological risk indices (PRI) in Cairo road dust indicate severe contamination with metals, particularly Pb, Zn, Cd, As, and Vanadium (V). The contamination factors (CF) indicated that these metals were present in higher concentrations than Ni, Cr, Co, and Ag, which also contaminated the road dust (Abdellatif and Saleh, 2012). This study aims to determine heavy metal content and spatial distribution to identify their spatial patterns in Cairo. Moreover, we aim to identify the possible main sources of individual metals in road dust using multivariate statistical analysis.

MATERIALS AND METHODS

1. Sample Collection

Road dust samples were gathered from various locations in Cairo, the capital of Egypt. These locations were selected based on their specific activities, including newly constructed highways, heavily trafficked roads, industrial roads, and roads connecting different areas of Cairo. The samples were collected from the western, southern, eastern, and northern parts of the city. The sampling process included the selection of the following locations: (i) five in the Western part, (ii) seven in the Southern part, (iii) four in the Eastern part, and (iv) three in the Northern part (**Table 1; Figure 1**). A total of 500 g of road dust particles were gathered at each sampling location using a pristine plastic dustpan and brush on non-porous areas of the road surface (sampling resolution: 1 × 1 m²). The particles were enclosed in self-sealing polyethylene bags and dispatched to the laboratory for further investigation. The samples were left to dry at room temperature for five days (Ferreira-Baptista and De Miguel,

2005). The samples were divided into four separate portions based on particle size using stainless steel mesh sieves with openings > 160 , $160-100$, $100-53$, and < 53 μm . This process was performed to eliminate any large debris. The resulting portions were then put into a fresh bag. The road dust samples with particle sizes less than 53 μm were analyzed for their heavy metal composition using inductively coupled plasma-mass spectroscopy. The samples underwent digestion according to the protocols established by the American Public Health Association (American Public Health *et al.*, 2005). In brief, 1 g of each dust sample was measured using an analytical balance and then transferred to a 100 mL glass beaker. The soil and wheat samples, which had been thoroughly dried at 105 $^{\circ}\text{C}$, were subjected to mineralization using a mixture of 65% nitric acid (Merck, Germany) and 36% hydrochloric acid (Merck, analytical grade, Germany) in a molar ratio of $1:3$. The mineralization process continued until complete digestion was achieved, after which the mixture was centrifuged at a speed of 6000 rpm for 10 min (Ibeto and Okoye, 2010). The samples were diluted to a volume of 100 mL using deionized water and then passed through filter sheets. The extracts underwent filtration using disposable 0.2 μm PTFE syringe filters (DISMIC-25HP, Advantec, Tokyo, Japan). The metal contents in these extracts were measured using inductively coupled plasma-mass spectroscopy (ICP-MS; iCAP, Thermo, Germany). The study incorporated certified reference materials (Merck, Germany). The recovery of metals fell within the permitted limits. The Qtegra program (USA) was utilized to calculate the average and relative standard deviation, as mandated by the APHA (American Public Health *et al.*, 2005). The samples underwent analysis to determine their level of Cr, Zn, As, Cd, Hg, Pb, Co, Bismuth (Bi), Ni, Cu, Gallium (Ga), Sr, Silver (Ag), Indium (In), Barium (Ba), and Iron (Fe).

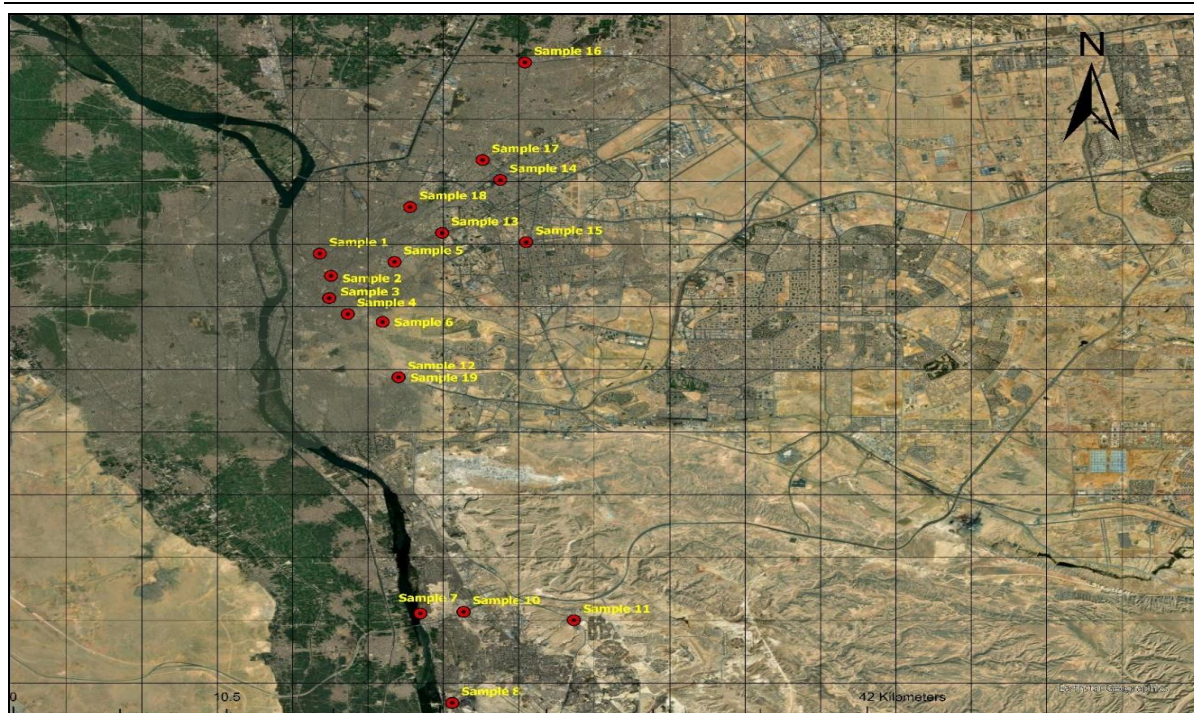


Figure 1. Map of Cairo City showing the number of the locations of the collected road dust samples

Table 1. Locations of the collected road dust samples in the study areas.

CARDINAL DIRECTION	SAMPL E NO	LOCATION	`N	E
West	1	Ramses Street	30°03'41.9"N	31°14'43.4"E
	2	Attaba	30°02'59.3"N	31°15'01.1"E
	3	Portsaedd street	30°02'16.6"N	31°14'58.3"E
	4	Salah EL-Din Street	30°01'46.1"N	31°15'27.7"E
	5	Waily Street	30°03'26.0"N	31°16'42.2"E
South	6	El Mokattam Road	30°01'31.0"N	31°16'23.2"E
	7	Tura	29°52'12.9"N	31°17'23.3"E
	8	The entrance to Cement Road	29°49'21.7"N	31°18'13.9"E
	9	Factories Road	29°47'37.5"N	31°18'59.0"E
	10	Middle Ring Road	29°52'16.0"N	31°18'32.0"E
	11	El-Nasr Road	29°51'59.9"N	31°21'27.5"E
	12	Al Aoutostrad	29°59'45.0"N	31°16'48.6"E
East	13	Salah Salem St	30°04'21.3"N	31°17'57.8"E
	14	Heliopolis	30°06'02.9"N	31°19'30.4"E
	15	Abbas El-Akkad	30°04'04.0"N	31°20'11.6"E
	16	Al Marj	30°09'47.8"N	31°20'09.6"E
North	17	El-Zaytoun El-Bahareya	30°06'419.0"N	31°19'02.3"E
	18	Masr We Al Sodan	30°05'10.9"N	31°17'07.0"E
	19	Mansheya El-Gamal	29°59'45.0"N	31°16'48.6"E

2. Single Pollution Indices

Index of Geo-accumulation (I_{geo})

Müller (1979) developed the I_{geo} by employing the subsequent equation to discern and depict metal pollution in soil and sediments: $I_{geo} = \log_2 (C_m / 1.5B_m)$, where C_m is the measured concentration of metal, and B_m is the geochemical background of the measured concentration (Bradl, 2005). Herein, we deployed the elemental concentrations in the upper continental crust (UCC) as the baseline values for the discovered heavy metals (Rudnick and Gao, 2003). A factor of 1.5 was used to include possible variation of background values due to lithogenic effects (Müller, 1979). The index of enrichment was: $I_{geo} < 0$ is unpolluted; $0 < I_{geo} < 1$ is unpolluted to moderately polluted; $1 < I_{geo} < 2$ is moderately polluted; $2 < I_{geo} < 3$ is moderately to strongly polluted; $3 < I_{geo} < 4$ is heavily polluted; $4 < I_{geo} < 5$ is heavily to strongly polluted; $5 < I_{geo}$ is extremely polluted (Muller, 1981).

Contamination Factor (CF)

Tomlinson et al. (1980) define CF as a parameter that quantifies the metal concentration in the sediments relative to a baseline value for each element.

$CF = C_s/C_b$, where C_b is the baseline concentration and C_s is the metal concentration in the study samples. Rudnick and Gao (2003) conducted the subsequent classification of CF, where the contamination levels were: $CF < 1$ as low; $CF < 3$ as moderate; $CF < 6$ as considerable; $CF > 6$ as high (Hakanson, 1980).

Enrichment Factor (EF)

$EF = (M_s/Fe_s) / (M_b/Fe_b)$, where M_b and Fe_b represent the target element and Fe content in the earth's crust, while M_s and Fe_s represent the target element and Fe content in each sample of road dust being analyzed. The heavy metals data was geochemically normalized to identify any abnormal metal concentrations in the conservation element (Xiong *et al.*, 2017; Mekky *et al.*, 2019). Herein, Fe was selected as a normalizing element to distinguish between natural and anthropogenic components (Loska *et al.*, 2003). The $EF < 2$ indicates that the metal is completely from the crust materials or natural processes, whereas $EF > 2$ indicates anthropogenic sources (Angelidis and Aloupi, 1997). The EF values < 2 indicate depletion to minimal enrichment, 2–5 indicate moderate enrichment, 5–20 indicate

significant enrichment, 20–40 indicate very high enrichment, and $EF > 40$ indicates extremely high enrichment.

Ecological Risk Factor (Er)

Hakanson (1980) proposed Er to measure the hazard contamination level in sediments. $Er = Tr \times CF$, where the factor depends on CF and the toxic-response factor (Tr). The Tr values were 2, 5, 5, 5, 1, 5, 10, 30, and 40 for Cr, Cu, Co, Ni, Zn, Pb, As, Cd, and Hg, respectively. The values of $Er < 40$ represent a low potential ecological risk, while values of Er between 40–80 represent a moderate potential ecological risk, and between 80–160 represent a considerable potential ecological risk. The values of Er between 160–320 represent a high potential ecological risk, and the values equal to or more than 320 represent a very high potential ecological risk.

Integrated Pollution Indices

Three integrated indices were used to assess the degree of pollution: the degree of contamination (DC), pollution load index (PLI), and pollution ecological risk index (PRI).

The Degree of Contamination (DC)

Hakanson (1980) defined the DC as the sum of all CFs and represented by the formula : $DC = \sum^n CF$, where DC values less than (n) indicate low value; $n \leq DC < 2n$ indicates moderate value; $2n \leq DC < 4n$ indicates considerable value; $DC > 4n$ indicates very high value (Caeiro *et al.*, 2005).

Pollution load index (PLI)

Tomlinson *et al.* (1980) suggested this PLI index and expressed the local community's concerns regarding the abundance of a certain element in the surrounding environment. Therefore, it serves as a rapid instrument for comparing the pollution levels in various areas (Adebowale *et al.*, 2009). $PLI = (CF1 \times CF2 \times CF3 \times \dots \times CFn)^{1/n}$, where (n) is the number of metals and CF is the contamination factor.

Pollution ecological risk index (PRI)

The heavy metals' PRI is quantified using the Er method. The PRI values were compared to the level of environmental contamination risk caused by Er metal (Hakanson, 1980).

RESULTS

1. Particle Size Distribution

Table 2 and Figures 2–5 display the particle size distribution, indicating that most samples have a grain size over 160 µm, accounting for almost 70% of the total. In the Western part of Cairo, the road dust particles were predominantly coarse in size, while in the Northern part, they were primarily finer, with a size of less than 160 µm.

Table 2. Particle size distribution of the collected road dust samples in the study areas.

CARDINAL DIRECTION	SAMPLE NO	SIEVE > 160 µM %	160 µM > SIEVE > 100 µM %	100 µM > SIEVE > 53 µM %	SIEVE < 53 µM %
West	1	80.17	10.86	6.07	2.9
	2	70.23	13.54	10.25	5.98
	3	82.38	6.35	6.84	4.43
	4	95.8	2.56	1.44	0.2
	5	84.02	6.69	6.58	2.71
South	6	57.18	10.92	21.4	10.5
	7	78.16	6.15	9.48	6.21
	8	73.81	10.4	12.41	3.38
	9	91.64	3.9	3	1.46
	10	90.58	4	3.29	2.03
	11	79.85	8.57	8.18	3.4
	12	78.24	10.77	8.34	2.65
East	13	82.35	7.74	7.5	2.41
	14	51.4	11.95	22.33	14.32
	15	72.32	9.8	10.82	7.06
	16	67.5	11	16.1	5.4
North	17	68.7	12.55	13.92	4.83
	18	54.3	16.7	21.56	7.44
	19	81	6.8	7.9	4.3

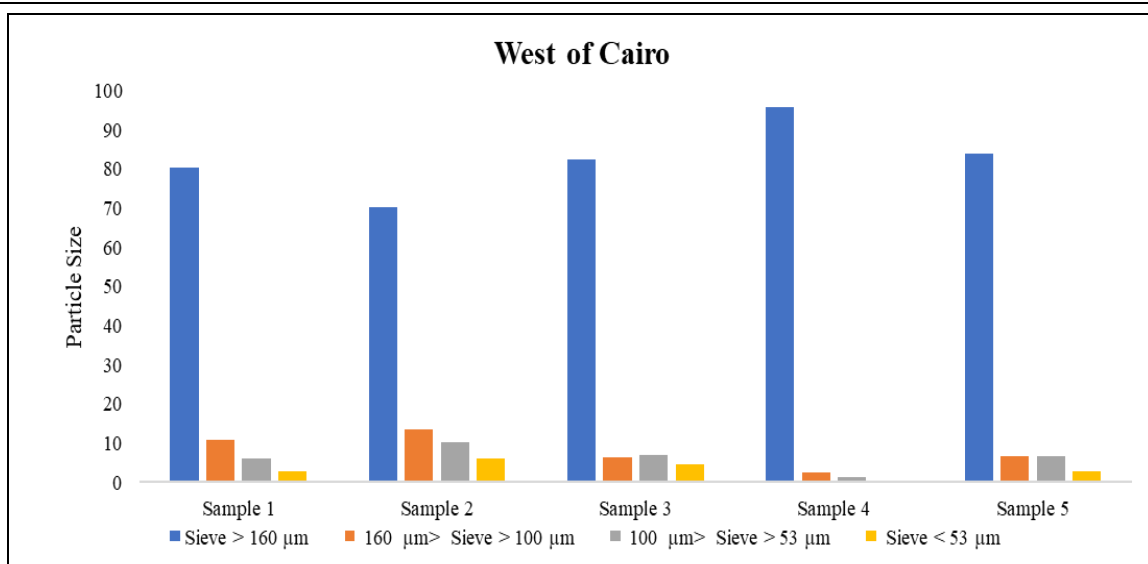


Figure 2. Particle size distribution of the collected road dust samples in the West of Cairo.

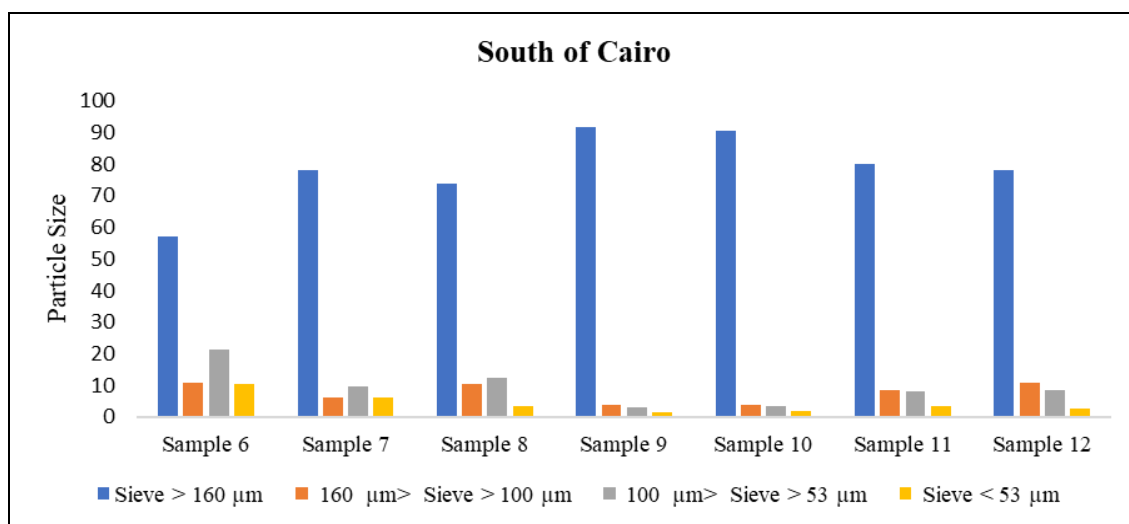


Figure 3. Particle size distribution of the collected road dust samples in the South of Cairo.

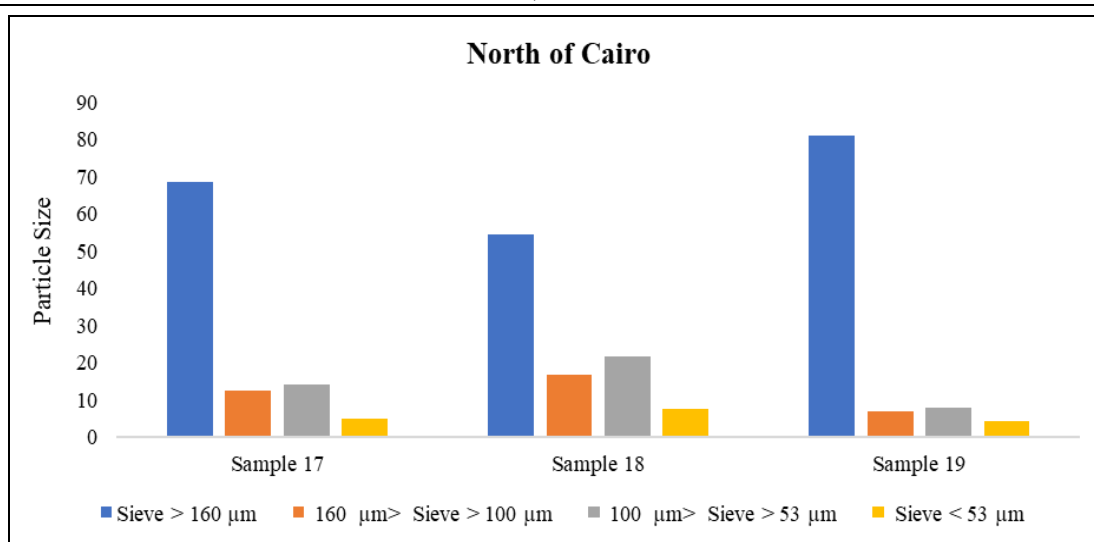


Figure 4. Particle size distribution of the collected road dust samples in the North of Cairo.

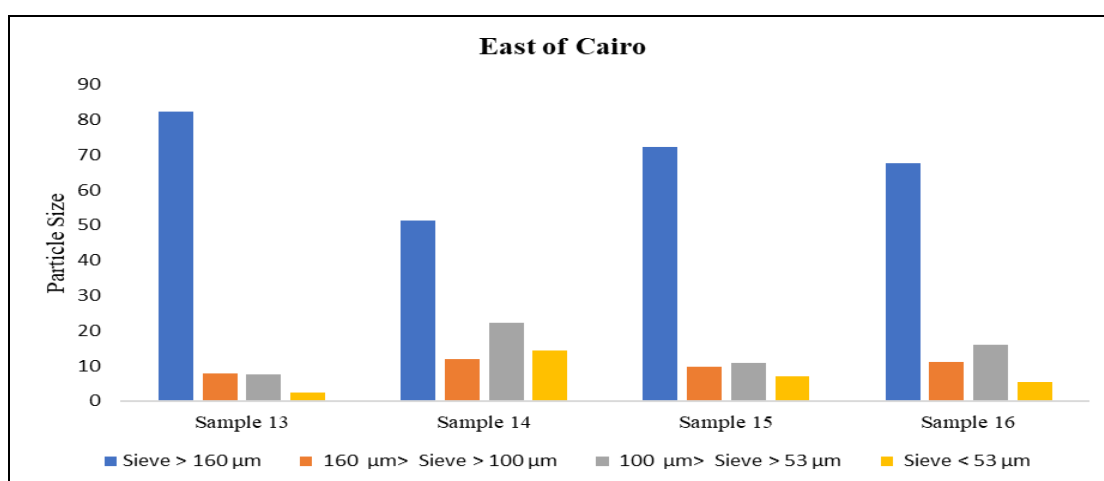


Figure 5. Particle size distribution of the collected road dust samples in the East of Cairo.

The analysis of the road dust samples in Cairo (**Tables 3–5; Figures 6–9**) revealed the presence of 16 heavy metals, including highly dangerous ones. Additionally, Bi was identified among the heavy metals (Wang *et al.*, 2019). It was found that road dust samples from the West, South, North, and East had varying levels of heavy metal content (**Tables 3–5**). Each study area exhibited significantly elevated levels of some possibly toxic metals,

including Zn, As, Cd, Hg, Pb, Co, In, Bi, and Cu. These metals originate from both natural and anthropogenic sources.

Table 3. Concentration of the heavy metals (ppm) for road dust of West Cairo.

CARDINAL DIRECTION	WEST				
Sample No	1	2	3	4	5
Cr	58.22	42.83	35.24	26.64	23.53
Zn	472.81	261.87	255.41	332.43	441.68
As	24.56	22.52	21.14	19.63	9.44
Cd	0.57	0.20	0.54	0.26	0.53
Hg	0.29	0.14	1.19	0.38	0.01
Pb	39.07	21.03	16.15	9.87	12.71
Co	2.16	3.36	2.02	1.14	2.58
Bi	60.69	30.17	12.36	7.70	8.04
Ni	19.08	20.11	14.89	11.95	16.80
Cu	130.14	63.12	85.96	44.92	466.39
Ga	1.53	0.99	0.77	0.42	0.74
Sr	3.37	2.79	3.03	3.44	3.90
Ag	9.25	4.15	92.19	20.88	1.45
In	2.84	0.38	0.20	0.15	0.05
Ba	21.19	4.35	44.24	33.59	2.00
Fe	217.25	289.12	294.01	182.71	323.43

Table 4. Concentration of the heavy metals (ppm) for road dust of South Cairo.

CARDINAL DIRECTION	SOUTH						
Sample No	6	7	8	9	10	11	12
Cr	64.26	32.87	29.42	75.20	63.51	13.48	23.02
Zn	410.95	275.57	223.65	365.42	325.22	182.73	388.68
As	22.71	25.13	23.38	18.91	21.02	8.75	9.69
Cd	2.07	0.55	0.23	0.32	2.62	0.13	0.38
Hg	0.60	0.77	1.40	1.22	5.47	0.26	0.07
Pb	19.73	10.86	14.48	12.02	30.70	8.41	1798.55
Co	4.09	2.42	2.14	3.55	3.06	0.99	2.28
Bi	8.92	6.36	6.65	9.07	396.36	20.40	14.38
Ni	410.22	80.57	18.60	21.09	18.21	7.13	15.06
Cu	210.15	96.69	38.91	59.44	69.71	17.60	372.60
Ga	1.33	0.79	0.95	1.56	13.11	0.23	0.64
Sr	4.41	3.94	4.31	4.11	3.73	3.07	3.67
Ag	4.49	5.53	13.81	25.79	134.50	2.63	1.51
In	0.23	0.09	0.23	0.14	49.34	0.10	0.07
Ba	11.24	8.88	3.52	19.53	6.27	3.35	3.09
Fe	409.95	348.53	350.25	877.10	434.78	129.33	309.11

Table 5. Concentration of the heavy metals (ppm) for road dust of East and North Cairo

CARDINAL DIRECTION	EAST				NORTH		
Sample No	13	14	15	16	17	18	19
Cr	34.20	52.11	36.96	22.65	43.16	36.00	24.29
Zn	300.77	316.65	270.13	255.33	264.98	293.46	249.82
As	14.74	25.87	25.72	16.96	24.11	14.82	11.57
Cd	0.23	0.33	0.29	0.44	0.38	0.46	0.23
Hg	0.28	0.92	0.51	0.69	0.62	0.19	0.71
Pb	9.54	8.62	9.68	21.32	14.55	11.84	11.93
Co	2.13	3.83	2.87	1.66	2.73	2.81	1.82
Bi	11.28	17.51	10.46	9.32	5.25	2.65	0.98
Ni	14.45	22.17	18.54	12.93	18.17	31.88	15.71
Cu	169.39	154.97	86.43	36.08	55.77	47.57	44.92
Ga	0.59	2.38	1.20	1.04	0.88	0.87	2.20
Sr	3.24	3.68	3.73	3.05	3.32	3.57	3.21
Ag	3.43	2.37	1.68	1.67	1.79	1.10	1.19
In	0.06	0.07	0.11	0.09	0.05	0.12	0.06
Ba	1.05	6.34	21.05	4.70	6.14	3.54	1.07
Fe	331.74	314.14	330.18	250.13	360.68	331.43	329.94

2. Single Pollution indices

The index of geo-accumulation (I_{geo}) (Tables 6–8; Figures 6–9) indicated that the road dust samples from all sides of Cairo exhibited varying degrees of pollution in terms of Cr, Zn, As, Cd, Hg, Pb, Co, Bi, Ni, Cu, Ga, Sr, Ag, In, Ba, and Fe. The pollution levels ranged from unpolluted to moderately contaminated, severely polluted, and extremely strongly polluted. Furthermore, the pollution levels range from moderate to low for Zn in all places, while Fe, Cr, Ga, Sr, Ag, Co, and Ba were not polluted. The Pb was uncontaminated in all samples except one sample, with an I_{geo} value of 6.14 (sample 11 from El-Nasr Road). The pollution level for Cu ranges from unpolluted to moderately polluted. All samples of Hg exhibit varying levels of pollution, ranging from unpolluted to very polluted, with an I_{geo} value of 6.19 (sample 9 from Factories Road). Furthermore, Bi showed severe pollution in most of the samples. Most road dust samples were not polluted for In, except those with I_{geo} values of 5.8 (sample 1 from Ramses Street) and 9.2 (sample 9 from Factories Road).

Table 6. The index of geo-accumulation (I_{geo}) of the heavy metals for road dust of West Cairo.

CARDINAL DIRECTION	WEST				
Sample No	1	2	3	4	5
Cr	-1.25	-1.69	-1.97	-2.37	-2.55
Zn	2.23	1.38	1.35	1.73	2.14
As	1.77	1.65	1.55	1.45	0.39
Cd	2.77	1.28	2.68	1.64	2.65
Hg	1.95	0.87	3.98	2.34	-3.22
Pb	0.62	-0.28	-0.66	-1.37	-1.00
Co	-3.59	-2.95	-3.68	-4.51	-3.33
Bi	7.98	6.97	5.69	5.00	5.07
Ni	-1.89	-1.81	-2.24	-2.56	-2.07
Cu	1.63	0.59	1.03	0.10	3.47
Ga	-4.10	-4.73	-5.10	-5.98	-5.15
Sr	-7.16	-7.43	-7.31	-7.13	-6.95
Ag	-3.10	-4.26	0.21	-1.93	-5.77
In	5.08	2.19	1.24	0.83	-0.61
Ba	-5.47	-7.76	-4.41	-4.81	-8.88
Fe	-7.92	-7.50	-7.48	-8.17	-7.34

Table 7. The index of geo-accumulation (I_{geo}) of the heavy metals for road dust of South Cairo.

CARDINAL DIRECTION	SOUTH						
Sample No	5	6	7	8	9	10	11
Cr	-1.10	-2.07	-2.23	-0.88	-1.12	-3.36	-2.58
Zn	2.03	1.46	1.15	1.86	1.69	0.86	1.95
As	1.66	1.80	1.70	1.39	1.55	0.28	0.43
Cd	4.62	2.70	1.44	1.94	4.96	0.68	2.17
Hg	3.01	3.37	4.22	4.02	6.19	1.78	-0.05
Pb	-0.37	-1.23	-0.82	-1.08	0.27	-1.60	6.14
Co	-2.67	-3.42	-3.60	-2.87	-3.08	-4.71	-3.51
Bi	5.22	4.73	4.79	5.24	10.69	6.41	5.90
Ni	2.54	0.19	-1.92	-1.74	-1.95	-3.30	-2.23
Cu	2.32	1.20	-0.11	0.50	0.73	-1.25	3.15
Ga	-4.30	-5.05	-4.79	-4.08	-1.00	-6.85	-5.35
Sr	-6.77	-6.93	-6.80	-6.87	-7.01	-7.29	-7.03
Ag	-4.15	-3.85	-2.53	-1.62	0.76	-4.92	-5.72
In	1.48	0.15	1.46	0.71	9.20	0.29	-0.17
Ba	-6.39	-6.73	-8.06	-5.59	-7.23	-8.14	-8.25
Fe	-7.00	-7.23	-7.23	-5.90	-6.92	-8.67	-7.41

Table 8. The index of geo-accumulation (I_{geo}) of the heavy metals for road dust of East and North Cairo.

CARDINAL DIRECTION	EAST				NORTH		
Sample No	13	14	15	16	17	18	19
Cr	-2.01	-1.41	-1.90	-2.61	-1.68	-1.94	-2.51
Zn	1.58	1.66	1.43	1.35	1.40	1.55	1.31
As	1.03	1.85	1.84	1.24	1.74	1.04	0.68
Cd	1.43	1.98	1.78	2.38	2.18	2.46	1.45
Hg	1.91	3.62	2.76	3.19	3.05	1.37	3.24
Pb	-1.42	-1.56	-1.40	-0.26	-0.81	-1.11	-1.10
Co	-3.61	-2.76	-3.18	-3.97	-3.25	-3.21	-3.83
Bi	5.55	6.19	5.45	5.28	4.45	3.46	2.03
Ni	-2.29	-1.67	-1.93	-2.45	-1.96	-1.15	-2.17
Cu	2.01	1.88	1.04	-0.22	0.41	0.18	0.10
Ga	-5.48	-3.46	-4.45	-4.66	-4.90	-4.92	-3.58
Sr	-7.21	-7.03	-7.01	-7.30	-7.18	-7.07	-7.22
Ag	-4.53	-5.07	-5.57	-5.57	-5.48	-6.18	-6.07
In	-0.48	-0.30	0.41	0.12	-0.84	0.57	-0.47
Ba	-9.80	-7.22	-5.48	-7.65	-7.26	-8.06	-9.78
Fe	-7.31	-7.38	-7.31	-7.71	-7.19	-7.31	-7.31

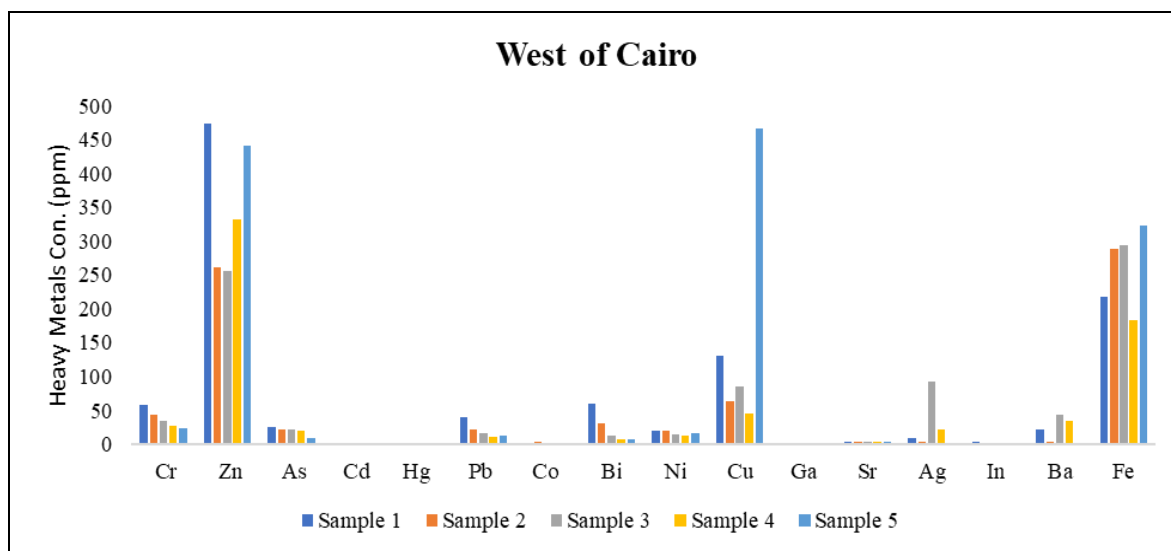


Figure 6. Index of geo-accumulation of the collected road dust samples in the West of Cairo.

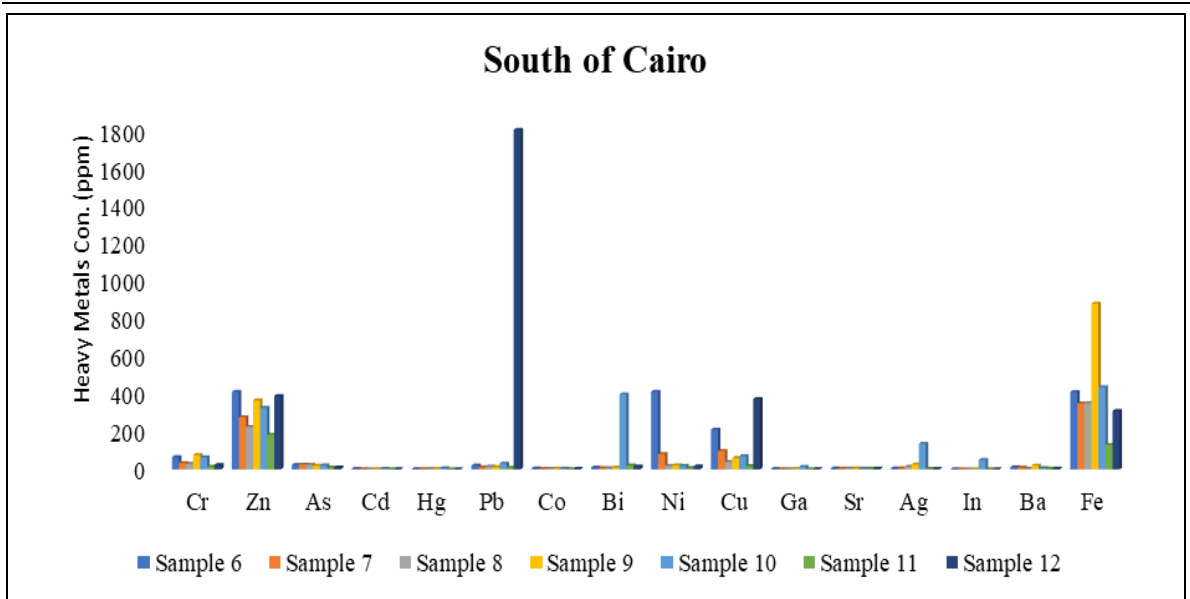


Figure 7. Index of geo-accumulation of the collected road dust samples in the South of Cairo.

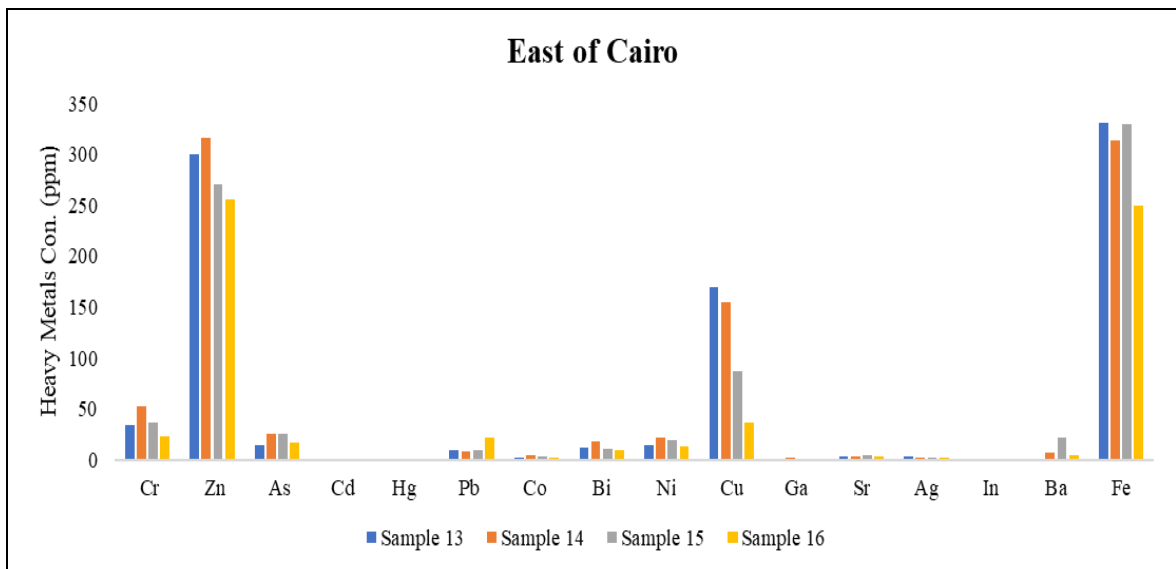


Figure 8. Index of geo-accumulation of the collected road dust samples in the East of Cairo.

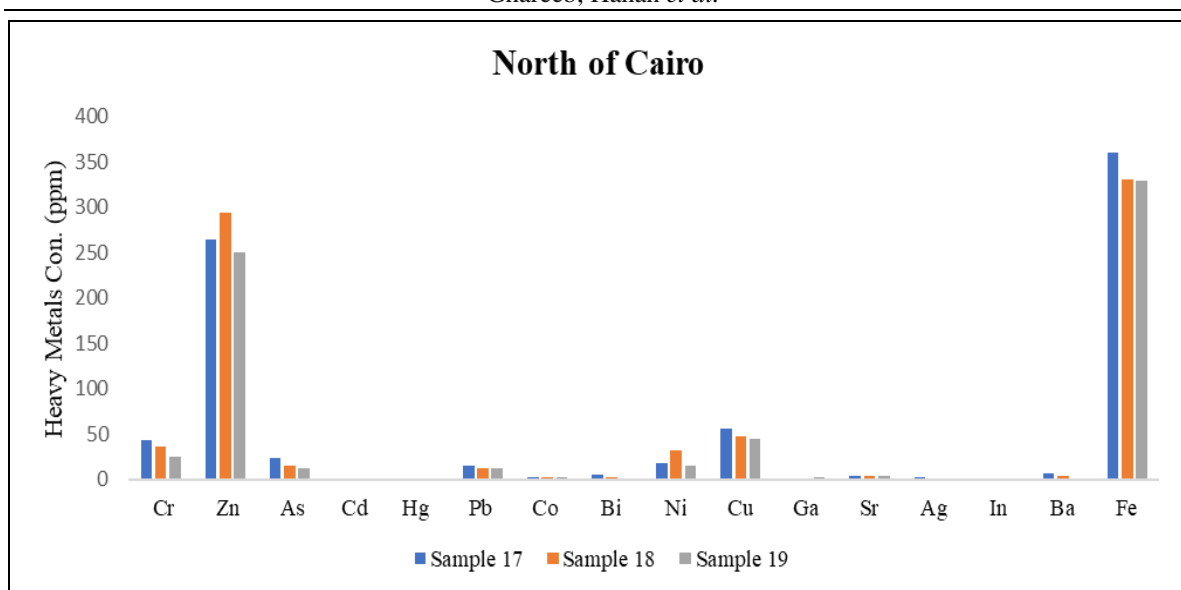


Figure 9. Index of geo-accumulation of the collected road dust samples in the North of Cairo.

Contamination Factor (CF)

The results for CF (**Tables 9–11; Figure 10**) indicated that all the road dust samples are heavily contaminated with Cd (CF = 46.74) and Hg (CF = 109.36), Bi (CF = 2477.25), Cu (CF = 16.66), Zn (CF = 7.06), Pb (CF = 105.80), In (CF = 881), Ni (CF = 8.73) when $CF > 6$. The samples demonstrated minimal contamination levels of Co, Cr, Ag, Ba, Sr, and Ga upon examination. Furthermore, the metals In, Ag, Cu, and Pb exhibited a moderate level of contamination. The Zn, As, and Cd metals in the samples exhibited significant contamination, whereas Bi and Hg were found to be extremely polluted.

Table 9. The contamination factor (CF), degree of contamination (DC), and pollution load index (PLI) of the heavy metals for road dust samples of West Cairo.

CARDINAL DIRECTION	WEST				
Sample No	1	2	3	4	5
Cr	0.63	0.47	0.38	0.29	0.26
Zn	7.06	3.91	3.81	4.96	6.59
As	5.12	4.69	4.40	4.09	1.97
Cd	10.20	3.63	9.63	4.67	9.40
Hg	5.81	2.74	23.71	7.58	0.16
Pb	2.30	1.24	0.95	0.58	0.75
Co	0.12	0.19	0.12	0.07	0.15
Bi	379.28	188.55	77.26	48.13	50.26
Ni	0.41	0.43	0.32	0.25	0.36
Cu	4.65	2.25	3.07	1.60	16.66
Ga	0.09	0.06	0.04	0.02	0.04
Sr	0.01	0.01	0.01	0.01	0.01
Ag	0.17	0.08	1.74	0.39	0.03
In	50.65	6.86	3.53	2.68	0.98
Ba	0.03	0.01	0.07	0.05	0.00
Fe	0.01	0.01	0.01	0.01	0.01
DC	466.53	215.13	129.07	75.39	87.62
PLI	0.95	0.52	0.77	0.47	0.33

Table 10. The contamination factor (CF), degree of contamination (DC), and pollution load index (PLI) of the heavy metals for road dust samples of South Cairo.

CARDINAL DIRECTION	SOUTH						
Sample No	6	7	8	9	10	11	12
Cr	0.70	0.36	0.32	0.82	0.69	0.15	0.25
Zn	6.13	4.11	3.34	5.45	4.85	2.73	5.80
As	4.73	5.23	4.87	3.94	4.38	1.82	2.02
Cd	37.01	9.73	4.07	5.77	46.74	2.40	6.73
Hg	12.10	15.48	27.90	24.36	109.36	5.16	1.45
Pb	1.16	0.64	0.85	0.71	1.81	0.49	105.80
Co	0.24	0.14	0.12	0.21	0.18	0.06	0.13
Bi	55.77	39.75	41.58	56.67	2477.26	127.52	89.87
Ni	8.73	1.71	0.40	0.45	0.39	0.15	0.32
Cu	7.51	3.45	1.39	2.12	2.49	0.63	13.31
Ga	0.08	0.05	0.05	0.09	0.75	0.01	0.04
Sr	0.01	0.01	0.01	0.01	0.01	0.01	0.01
Ag	0.08	0.10	0.26	0.49	2.54	0.05	0.03
In	4.18	1.66	4.14	2.45	881.00	1.84	1.34
Ba	0.02	0.01	0.01	0.03	0.01	0.01	0.00
Fe	0.01	0.01	0.01	0.03	0.01	0.00	0.01
DC	138.45	82.47	89.32	103.59	3532.47	143.03	227.11
PLI	0.98	0.59	0.52	0.77	2.20	0.25	0.54

Table 11. The contamination factor (CF), degree of contamination (DC), and pollution load index (PLI) of the heavy metals for road dust of East and North of Cairo.

CARDINAL DIRECTION	EAST				NORTH		
Sample No	13	14	15	16	17	18	19
Cr	0.37	0.57	0.40	0.25	0.47	0.39	0.26
Zn	4.49	4.73	4.03	3.81	3.95	4.38	3.73
As	3.07	5.39	5.36	3.53	5.02	3.09	2.41
Cd	4.03	5.93	5.13	7.80	6.80	8.23	4.10
Hg	5.65	18.39	10.16	13.71	12.42	3.87	14.19
Pb	0.56	0.51	0.57	1.25	0.86	0.70	0.70
Co	0.12	0.22	0.17	0.10	0.16	0.16	0.11
Bi	70.49	109.44	65.41	58.23	32.84	16.55	6.14
Ni	0.31	0.47	0.39	0.28	0.39	0.68	0.33
Cu	6.05	5.53	3.09	1.29	1.99	1.70	1.60
Ga	0.03	0.14	0.07	0.06	0.05	0.05	0.13
Sr	0.01	0.01	0.01	0.01	0.01	0.01	0.01
Ag	0.06	0.04	0.03	0.03	0.03	0.02	0.02
In	1.08	1.22	1.99	1.63	0.84	2.22	1.08
Ba	0.00	0.01	0.03	0.01	0.01	0.01	0.00
Fe	0.01	0.01	0.01	0.01	0.01	0.01	0.01
DC	96.34	152.61	96.85	92.00	65.85	42.07	34.83
PLI	0.37	0.59	0.52	0.41	0.44	0.38	0.30

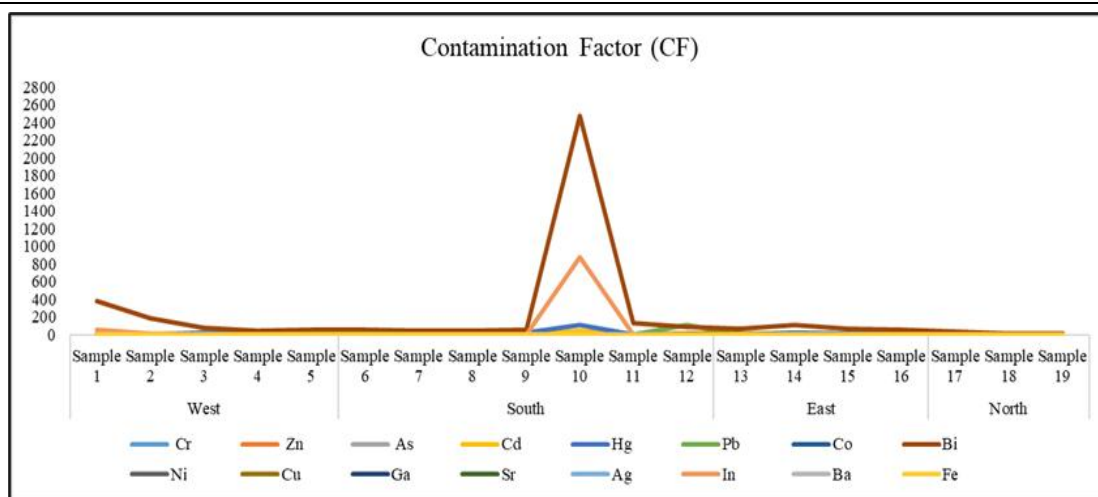


Figure 10. The contamination factor (CF) of the heavy metals for road dust of Cairo.

Enrichment Factor (EF)

The EF analysis of the study's road dust samples (**Tables 12–14**) showed that all the road dust samples were extremely high enrichment with the heavy metals Zn, As, Cd, Bi, and Pb (except in sample 6, where it is high enrichment), Cu and In. The samples demonstrated that the heavy metals Cr and Ni varied between very high enrichment to extremely high enrichment. Furthermore, the metals Ga and Ag vary from moderate to extremely high enrichment, and Sr exhibited depletion to minimal enrichment. The Ba metal in the samples varied from depletion to minimal enrichment to significant enrichment.

Table 12. The enrichment factor of the heavy metals for road dust samples of West Cairo.

CARDINAL DIRECTION	WEST				
Sample No	1	2	3	4	5
Cr	103.41	57.17	46.25	56.27	28.07
Zn	1153.15	479.92	460.28	964.02	723.58
As	836.07	576.16	531.82	794.74	215.81
Cd	1666.93	446.16	1163.27	906.78	1031.85
Hg	948.82	336.68	2862.82	1472.89	17.70
Pb	375.51	151.87	114.72	112.85	82.07
Co	20.37	23.85	14.11	12.76	16.38
Bi	61978.15	23152.30	9329.09	9351.63	5516.49
Ni	66.33	52.53	38.26	49.39	39.23
Cu	759.51	276.79	370.68	311.68	1828.28
Ga	14.25	6.95	5.29	4.63	4.63
Sr	1.72	1.07	1.14	2.09	1.34
Ag	28.53	9.62	210.02	76.56	3.01
In	8276.30	842.84	426.62	519.79	107.75
Ba	5.51	0.85	8.51	10.39	0.35

Table 13. The enrichment factor of the heavy metals for road dust samples of South Cairo.

CARDINAL DIRECTION	SOUTH						
Sample No	6	7	8	9	10	11	12
Cr	60.49	36.39	32.42	33.08	56.36	40.22	28.74
Zn	531.13	418.93	338.33	220.75	396.33	748.61	666.23
As	409.72	533.21	493.68	159.42	357.48	500.64	231.92
Cd	3204.69	991.48	412.22	233.42	3816.71	658.82	773.35
Hg	1047.53	1577.12	2828.24	985.76	8929.57	1416.73	166.71
Pb	100.49	65.09	86.36	28.63	147.44	135.79	12150.18
Co	20.48	14.26	12.53	8.30	14.45	15.68	15.14
Bi	4828.99	4048.26	4214.37	2293.75	202268.35	35003.21	10320.91
Ni	755.81	174.61	40.11	18.16	31.63	41.67	36.81
Cu	649.92	351.73	140.84	85.93	203.28	172.54	1528.26
Ga	6.60	4.62	5.48	3.60	61.15	3.58	4.21
Sr	1.19	1.26	1.37	0.52	0.95	2.63	1.32
Ag	7.33	10.63	26.41	19.70	207.21	13.62	3.28
In	361.83	169.57	419.64	99.28	71933.55	504.08	153.61
Ba	1.55	1.44	0.57	1.26	0.82	1.46	0.56

Table 14. The enrichment factor of the heavy metals for road dust samples of East and North Cairo.

CARDINAL DIRECTION	EAST				NORTH		
Sample No	13	14	15	16	17	18	19
Cr	39.77	64.01	43.20	34.94	46.18	41.91	28.41
Zn	480.38	534.09	433.49	540.85	389.26	469.16	401.20
As	328.54	609.18	576.07	501.54	494.36	330.67	259.34
Cd	431.64	670.56	551.97	1107.10	669.35	881.97	441.17
Hg	604.09	2077.88	1092.53	1945.73	1222.39	414.63	1527.18
Pb	60.03	57.32	61.19	178.00	84.27	74.62	75.50
Co	13.19	24.99	17.81	13.60	15.55	17.42	11.35
Bi	7543.64	12366.95	7032.24	8264.90	3232.30	1773.13	660.28
Ni	32.91	53.31	42.42	39.05	38.05	72.64	35.96
Cu	647.38	625.46	331.89	182.87	196.03	181.99	172.61
Ga	3.60	15.37	7.39	8.41	4.95	5.31	13.50
Sr	1.08	1.30	1.25	1.35	1.02	1.20	1.08
Ag	6.93	5.05	3.41	4.47	3.32	2.21	2.41
In	115.25	137.87	213.85	231.77	82.55	238.23	116.23
Ba	0.18	1.14	3.60	1.06	0.96	0.60	0.18

Ecological Risk

The analysis of the study samples (**Table 15**) revealed that Cairo exhibited a significantly elevated ecological risk with regard to Cd (Er = 1402.34 sample 10 from Middle Ring Road), which contradicts the findings of I_{geo} . Furthermore, the measured Co, Cr, Cu, Ni, and Zn concentrations exhibited a minimal ecological risk within the designated study region. Metals such as As, Ni, Cu, and Pb had a significant potential for causing ecological risk.

Table 15. The ecological risk factor (Er) and pollution ecological risk index (PRI) of the heavy metals for road dust of Cairo.

CARDINAL DIRECTION	SAMPLE NO	CR	ZN	AS	CD	PB	CO	NI	CU	HG	PRI
West	1	1.27	7.06	51.16	306.03	2.03	0.62	2.03	23.24	232.26	625.69
	2	0.93	3.91	46.92	109.01	2.14	0.97	2.14	11.27	109.68	286.97
	3	0.77	3.81	44.04	289.03	1.58	0.58	1.58	15.35	948.40	1305.15
	4	0.58	4.96	40.90	140.01	1.27	0.33	1.27	8.02	303.23	500.57
	5	0.51	6.59	19.66	282.03	1.79	0.75	1.79	83.28	6.45	402.85
South	6	1.40	6.13	47.31	1110.23	43.64	1.18	43.64	37.53	483.87	1774.94
	7	0.71	4.11	52.35	292.03	8.57	0.70	8.57	17.27	619.36	1003.67
	8	0.64	3.34	48.71	122.01	1.98	0.62	1.98	6.95	1116.15	1302.36
	9	1.63	5.45	39.39	173.01	2.24	1.03	2.24	10.61	974.21	1209.82
	10	1.38	4.85	43.78	1402.34	1.94	0.88	1.94	12.45	4374.56	5844.12
	11	0.29	2.73	18.24	72.00	0.76	0.29	0.76	3.14	206.45	304.66
	12	0.50	5.80	20.19	202.02	1.60	0.66	1.60	66.54	58.06	356.98
East	13	0.74	4.49	30.70	121.01	1.54	0.62	1.54	30.25	225.81	416.69
	14	1.13	4.73	53.91	178.01	2.36	1.11	2.36	27.67	735.49	1006.76
	15	0.80	4.03	53.58	154.01	1.97	0.83	1.97	15.43	406.45	639.09
	16	0.49	3.81	35.34	234.02	1.38	0.48	1.38	6.44	548.39	831.72
North	17	0.94	3.95	50.23	204.02	1.93	0.79	1.93	9.96	496.78	770.53
	18	0.78	4.38	30.87	247.02	3.39	0.81	3.39	8.50	154.84	453.98
	19	0.53	3.73	24.10	123.01	1.67	0.53	1.67	8.02	567.75	731.00

DISCUSSION

The diverse range of particle sizes and chemical composition observed in the road dust samples of Cairo has been demonstrated to be mostly attributed to the emissions and weathering processes occurring in the city (Abdellatif and Saleh, 2012; Hassan *et al.*, 2019; Mohammed and Saleh, 2020). Our study revealed a significant variation in particle size differentiation among the road dust samples. Conducting particle size analysis of road dust and comparing it to a complete road dust sample using chemical analyses offers numerous advantages. The present research focused on screening particles larger than 53 μm to determine the concentration of heavy metals present. Consequently, finer particles were found to tend to have higher concentrations of heavy metals (Lanzerstorfer and Logiewa, 2019).

In certain road dust samples, particularly in the western region, the concentration of certain metals, such as Bi = 60.69 ppm in sample 1 from Ramses Street, showed a considerable rise, likely due to urbanization, small industries, and high population density. Ag content in sample 3 Portsaid Street was 92.19 ppm, which may be attributed to the small industries of silver. Cu concentration in sample 5 Waily Street was 466.39 ppm, possibly linked to urban activities. In South Cairo, on Al Aoutostrad sample 12, the concentrations of metals were Pb = 1798.55 ppm and Cu = 372.60 ppm due to heavy traffic and inadequate road maintenance. In sample 6, on a highway with significant traffic and poor road maintenance, Ni = 410.22 ppm and Cu = 210.15 ppm were detected. Sample 10 showed Bi = 396.36 ppm, Ag = 134.50 ppm, and In = 49.34 ppm, possibly influenced by nearby small industries. The concentration of FE in sample 9 was 877.10 ppm, which was closely linked to the extent of anthropogenic.

There was a significant decrease in the levels of heavy metals, namely Pb, Fe, Cr, and Co, which had previously increased 10 years ago and were mentioned in previous research studies (Abdellatif and Saleh, 2012). However, Bi was not mentioned in those studies. In this current study, Bi was the most polluted metal in all samples collected around Cairo. This is because the geochemical background concentration of Bi is 0.6 ppm, as mentioned in UCC (Rudnick and Gao, 2003), but the concentrations found in road dust samples significantly exceeded this value. Although there is no study proving the hazardous effects of Bi in Pb or Zn ores, it is clear that most road dust samples show depletion and low concentrations of Pb or Zn, possibly because of anthropogenic activities (Wang et al., 2019). In general, road dust concentrations of Bi in this study were higher than those in the ordinary crust (Rudnick and Gao, 2003).

A comprehensive analysis was conducted on previous research papers, predominantly published within the last two decades. These papers encompassed data from over 5000 sampling sites in 61 cities across 21 countries. The objective of this analysis was to obtain a deeper understanding of the present situation and potential hazards related to heavy metals found in road dust in major urban areas. This study comprehensively examines the concentration, sources, dispersion, health hazards, collection methods, and analytical

approaches employed in worldwide urban areas to investigate heavy metal content in road dust. The study conducted by (Shahab et al., 2023) revealed the global occurrence of Cd, Zn, and Cu in various urban road dust samples. In contrast, the current investigation focuses on detecting Bi, Hg, Cd, and In. While the I_{geo} values in a previous study have indicated increased Pb contamination (Safar and Labib, 2010), this study clarified that the highest contamination levels were observed for Bi, followed by Hg, Cd, Cu, and Zn. Notably, no significant contamination was observed for Pb, except in one sample where regular cleaning was not performed.

The calculation of single pollution indices, such as I_{geo} , reveals the following order of pollutants from highest to lowest concentration: Bi > Hg > Cd > Cu > Zn > In > As > Pb > Ni > Cr\Co\Ag > Ga > Sr > Fe. The following order represents the metals with the highest contamination levels from highest to lowest: Bi, Hg, Cd, As, Zn, and In. This order indicates no contamination for Ni, Cr, Co, and Pb, as these are some of the important heavy metals. The EF in this study reveals that while the I_{geo} was low for most of the metals, the EF was above 40, indicating a significant enrichment of the metal.

CONCLUSION AND RECOMMENDATION

The study reveals that human activities are the primary cause of elevated levels of heavy metals in road dust samples, with Bi concentrations significantly higher than natural levels found in the continental crust. This suggests significant utilization of Bi in various industries and contexts, resulting in gradual contamination. The ecological risk assessment indicates that road dust poses varying degrees of ecological harm, ranging from low to high potential. The metals As and Cd have increased compared to other metals, causing related risks. The environmental steps revealed that the concentration of heavy metals, including Pb and Zn, remains below permissible limits. However, the rising Bi levels should be considered a warning sign due to its extensive use without proper care.

The research highlights the need for ongoing surveillance and control of heavy metal substances and the escalating concentration of Bi. The Greater Cairo Air Pollution Management and Climate Change Project aligns with Egypt's Sustainable Development

Strategy, Egypt Vision 2030, to support Egypt's initiatives in decreasing climate pollutants and air pollution emissions. The project aims to assist Egypt in achieving its 2030 emission reduction goals and advancing its major environmental objective of reducing particulate matter pollution by half.

The research findings will aid in establishing a road dust management program by prioritizing Bi, Hg, Cd, Cu, Zn, In, and As while limiting input from other sources. Further research is needed on the bioavailability and mobilization of road dust, the efficacy of current street cleaning technologies, the aerodynamic properties of road particles, and seasonal variations in metal levels.

Consent for publication

All authors approved the manuscript for publication.

Disclosure statement

The authors declared no conflicts of interest.

Availability of data

All the data in this study are available in the manuscript.

Funding

This work received no funding.

Author contributions

Fayza S. Hashem and R.M. Maree designed the research; Hanan Hegazy performed all experiments; Fayza S. Hashem and Hanan Hegazy analyzed the data; Hanan Hegazy and Fayza S. Hashem wrote and edited the manuscript.

REFERENCES

- Abbasi, S., Keshavarzi, B., Moore, F., Delshab, H., Soltani, N., & Sorooshian, A. (2017). Investigation of microrubbers, microplastics and heavy metals in street dust: a study in Bushehr city, Iran. *Environmental earth sciences*, 76, 1-19.
- Abdellatif N., Saleh I. (2012). Heavy metals contamination in roadside dust along major roads and correlation with urbanization activities in Cairo, Egypt. *Journal of American Science*, 8(6), 379-389.
- Adebowale K.O., Agunbiade F.O., Olu-Owolabi B.I. (2009). Trace metal concentrations, site variations and partitioning pattern in water and bottom sediments from coastal area: a case study of Ondo coast, Nigeria. *Environmental Research Journal*, 3, 46-59.
- American Public Health A., Eaton A.D., American Water Works A., Water Environment F. (2005). *Standard methods for the examination of water and wastewater*, Washington, D.C., APHA-AWWA-WEF Washington, D.C.
- Angelidis M.O., Aloupi M. (1997). Assessment of Metal Contamination in Shallow Coastal Sediments Around Mytilene Greece. *Int. J. Environ. Anal. Chem.*, 68, 281-293.
- Bradl H. (2005). *Heavy Metals in the Environment: Origin, Interaction and Remediation*, Amsterdam/Boston, Elsevier Academic Press.
- Caeiro S., Costa M.H., Ramos T., Fernandes F., Silveira N., Coimbra A., Medeiros G., Painho M. (2005). Assessing heavy metal contamination in Sado Estuary sediment: An index analysis approach. *Ecological indicators*, 5(2), 151-169.
- Calvert J.G. (1990). Glossary of atmospheric chemistry terms (Recommendations 1990). *Pure and applied chemistry*, 62, 2167-2219.
- Duong T.T.T., Lee B.-K. (2011). Determining contamination level of heavy metals in road dust from busy traffic areas with different characteristics. *Journal of environmental management*, 92, 554-562.
- El-Anwar E., Samy Y., Salman S. (2018). Heavy metals hazard in Rosetta Branch sediments, Egypt. *Journal of Materials and Environmental Science*, 9, 2142-2152.
- Ferreira-Baptista L., De Miguel E. 2005. Geochemistry and risk assessment of street dust in Luanda, Angola: A tropical urban environment. *Atmos. Environ.*, 39, 4501-4512.
- Gabarrón M., Faz A., Acosta J.A. 2017. Effect of different industrial activities on heavy metal concentrations and chemical distribution in topsoil and road dust. *Environmental Earth Sciences*, 76, 129.
- Hakanson L. (1980). An ecological risk index for aquatic pollution control. a sedimentological approach. *Water Research*, 14, 975-1001.

- Han X., Lu X., Wu Y. 2017. Health risks and contamination levels of heavy metals in dusts from parks and squares of an industrial city in semi-arid area of China. *International Journal of Environmental Research and Public Health*, 14(8), 886.
- Hassan S., Mohammed A., Khoder M. (2019). Characterization and Health Risk Assessment of Human Exposure to PAHs in Dust Deposited on Leaves of Street Trees in Egypt. *Polycyclic Aromatic Compounds*, 40, 1-15.
- Ibeto C., Okoye C.O. (2010). High levels of heavy metals in blood of the urban population in Nigeria. *Research Journal of Environmental Sciences*, 4, 371-382.
- Lanzerstorfer C., Logiewa A. 2019. The upper size limit of the dust samples in road dust heavy metal studies: Benefits of a combined sieving and air classification sample preparation procedure. *Environmental Pollution*, 245, 1079-1085.
- Loska K., Wiechula D., Barska B., Cebula E., Chojnecka A. (2003). Assessment of arsenic enrichment of cultivated soils in Southern Poland. *Polish Journal of Environmental Studies*, 12, 187-192.
- Mekky H., El-Anwar E., Salman S., Elnazer A., Ibrahim W., Asmoay A. (2019). Evaluation of Heavy Metals Pollution by using pollution indices in the Soil of Assiut District, Egypt. *Egyptian Journal of Chemistry*, 62(9), 1673-1683.
- Meza-Figueroa D., De La O-Villanueva M., De La Parra M.L. 2007. Heavy metal distribution in dust from elementary schools in Hermosillo, Sonora, México. *Atmos. Environ.*, 41, 276-288.
- Mitra S., Chakraborty A.J., Tareq A.M., Emran T.B., Nainu F., Khusro A., Idris A.M., Khandaker M.U., Osman H., Alhumaydhi F.A., Simal-Gandara J. (2022). Impact of heavy metals on the environment and human health: Novel therapeutic insights to counter the toxicity. *Journal of King Saud University - Science*, 34, 101865.
- Mohammed A., Saleh I. (2020). A review of sulfur dioxide and particulate matter (PM_{2.5} and PM₁₀) in greater Cairo, Egypt. *Int. J. Biosens. Bioelectron*, 6, 56-68.
- Muller G. (1981). The heavy metal content of the sediments of the Neckar and its tributaries: an inventory. *Chem. Zeitung*, 105, 157-164.
- Müller G. (1979). Schwermetalle in den Sedimenten des Rheins-Veränderungen seit 1971.
- Olmedo P., Goessler W., Tanda S., Grau-Perez M., Jarmul S., Aherrera A., Chen R., Hilpert M., Cohen Joanna E., Navas-Acien A., Rule Ana M. (2018). Metal concentrations in e-cigarette liquid and aerosol samples: The contribution of metallic coils. *Environmental health perspectives*, 126(2), 027010.
- Ramírez O., Sánchez De La Campa A.M., Amato F., Moreno T., Silva L.F., De La Rosa J.D. (2019). Physicochemical characterization and sources of the thoracic fraction of road dust in a Latin American megacity. *Science of the Total Environment*, 652, 434-446.

- Rudnick R.L. and Gao S. (2003). Composition of the Continental Crust. *In: Holland, H. D. & Turekian, K. K. (eds.) Treatise on Geochemistry*. Oxford: Pergamon.
- Safar Z.S. and Labib M.W. (2010). Assessment of particulate matter and lead levels in the Greater Cairo area for the period 1998–2007. *Journal of Advanced Research*, 1, 53-63.
- Shahab A., Hui Z., Rad S., Xiao H., Siddique J., Huang L.L., Ullah H., Rashid A., Taha M.R., Zada N. (2023). A comprehensive review on pollution status and associated health risk assessment of human exposure to selected heavy metals in road dust across different cities of the world. *Environmental geochemistry and health*, 45(3), 585-606.
- Silander D. (2019). The European Commission and Europe 2020: Smart, sustainable and inclusive growth. *Smart, sustainable and inclusive growth*, 2-35.
- Tomlinson D.L., Wilson J.G., Harris C.R., Jeffrey D.W. (1980). Problems in the assessment of heavy-metal levels in estuaries and the formation of a pollution index. *Helgoländer Meeresuntersuchungen*, 33, 566-575.
- Trujillo-González J.M., Torres-Mora M.A., Keesstra S., Brevik E.C., Jiménez-Ballesta R. (2016). Heavy metal accumulation related to population density in road dust samples taken from urban sites under different land uses. *Sci. Total Environ.*, 553, 636-642.
- Wang R., Li H., Sun H. 2019. Bismuth: Environmental Pollution and Health Effects. *Encyclopedia of Environmental Health*, 415 - 423.
- Wang X., Liu E., Lin Q., Liu L., Yuan H., Li Z. (2020). Occurrence, sources and health risks of toxic metal(loid)s in road dust from a mega city (Nanjing) in China. *Environmental pollution*, 263, 114518.
- Xiong Q., Zhao W., Zhao J., Zhao W., Jiang L. (2017). Concentration Levels, Pollution Characteristics and Potential Ecological Risk of Dust Heavy Metals in the Metropolitan Area of Beijing, China. *International journal of environmental research and public health*, 14(10), 1159.
- Yang Y.-W., Liou S.-H., Hsueh Y.-M., Lyu W.-S., Liu C.-S., Liu H.-J., Chung M.-C., Hung P.-H., Chung C.-J. (2018). Risk of Alzheimer's disease with metal concentrations in whole blood and urine: A case–control study using propensity score matching. *Toxicology and applied pharmacology*, 356, 8-14.

التوصيف الجيوكيميائي للعناصر الفلزية الثقيلة وتقييم المخاطر البيئية

لغبار الطرق في القاهرة، مصر

حنان حجازي غريب⁽¹⁾ - فائزة سيد هاشم⁽²⁾ - رجب محسوب عبد الله مرعي⁽³⁾ - محمود إبراهيم الحويحي⁽¹⁾
(1) قسم العلوم الأساسية البيئية، كلية الدراسات العليا والبحوث البيئية، جامعة عين شمس (2) قسم الكيمياء، كلية العلوم، جامعة عين شمس، القاهرة، مصر (3) إدارة الوقاية من الإشعاع، هيئة الطاقة الذرية، مصر

المستخلص

يعد تلوث غبار الطرق في المناطق الحضرية مشكلة مهمة تساهم في تلوث الغلاف الجوي وتخزين الملوثات مثل العناصر الثقيلة. تهدف هذه الدراسة إلى تحديد محتوى العناصر الثقيلة والتوزيع المكاني لغبار الطرق في القاهرة، وهي منطقة ذات نشاط بشري متزايد، وتحديد المصادر الرئيسية المحتملة للعناصر الفردية باستخدام التحليل الإحصائي متعدد المتغيرات. استخدمت دراستنا التحليل الطيفي لكتلة البلازما المقترنة حثيًا (ICP-MS) لتقييم 15 عنصراً ثقيلاً منها، بما في ذلك الكروم (Cr) والزنك (Zn) والزرنيخ (As) والكاديوم (Cd) والزرنيق (Hg) والرصاص (Pb) والكوبالت (Co) والبروم (Bi) والنيكل (Ni) والنحاس (Cu) والغالسيوم (Ga) والسترونشيوم (Sr) والفضة (Ag) والإنديوم (In) والباريوم (Ba) والحديد (Fe) في العينات. تم استخدام مؤشرات التراكم الجغرافي المختلفة، وعوامل التلوث، ودرجة التلوث، ومؤشر حمل التلوث، وعامل التخصيب، ومؤشر خطر التلوث البيئي لتقييم درجة التلوث. أظهرت النتائج أن متوسط تراكيز العناصر الثقيلة الرئيسية كان 1798.55، 396.3، 410.22، 466.39، 472.81 جزء في المليون للرصاص، Cu، Ni، Bi، Zn، على التوالي. كان التوزيع المكاني للعناصر الثقيلة خاصاً بالموقع، مع مستويات ثنائية عالية بسبب الأنشطة الصناعية المكثفة. انخفضت درجة التلوث بالترتيب Cu > As > In > Zn > Cd > Hg > Bi وتتراوح العناصر الثقيلة من غير الملوثة إلى شديدة التلوث. تشير الدراسة إلى أنه بما أن الزموت يحل محل الرصاص في الصناعة التحويلية لأنه يشكل أخطار أقل، فيجب معرفة المستجيب السام (Tr) فيما يتعلق بالإثراء الكبير له.

الكلمات المفتاحية: غبار الطريق، مؤشرات التلوث، عناصر ثقيلة، التقييم البيئي، الزموت